HHS Public Access

Author manuscript

J Neuroimaging. Author manuscript; available in PMC 2018 September 01.

Published in final edited form as:

J Neuroimaging. 2017 September ; 27(5): 453–460. doi:10.1111/jon.12432.

Spatial co-registration of functional near-infrared spectroscopy to brain MRI

Michelle Chen[1], **Helena M. Blumen**[2], **Meltem Izzetoglu**[3], and **Roee Holtzer**[1,2]

[1]Ferkauf Graduate School of Psychology, Yeshiva University, Bronx, NY

[2]Albert Einstein College of Medicine, Yeshiva University, Bronx, NY

[3]School of Biomedical Engineering, Science, and Health Systems, Drexel University, Philadelphia, PA

Abstract

BACKGROUND AND PURPOSE—Traditional neuroimaging techniques restrict movement and make it difficult to study the processes that require oral, upper limb, or lower limb motor execution. Functional Near-Infrared Spectroscopy (fNIRS) is an optical neuroimaging modality that measures brain oxygenation and permits movement during data acquisition. A key limitation of fNIRS, however, is the lack of a standard method to co-register quantitative fNIRS measurements to structural images such as MRI. Additionally, fNIRS-MRI co-registration studies have not been reported in older adults.

METHODS—fNIRS and structural MRI were acquired from 30 non-demented older adults. Sixteen fNIRS channels that assess hemodynamic changes in the prefrontal cortex (PFC; an area crucial in various age-related processes) were co-registered to structural MRI. Vitamin E capsules were used to mark the locations of fNIRS detectors and light sources on the scalp. We used the balloon-inflation algorithm to project fNIRS channel locations on the scalp to underlying cortical surface.

RESULTS—We provide coordinates for the 16 fNIRS channels in the PFC on the cortical surface in both MNI and Talairach spaces, with minimal variability that is within the spatial resolution of our fNIRS system.

CONCLUSIONS—Our study provides useful spatial information for standalone fNIRS data in future studies, particularly investigations in age-related processes.

Keywords

fNIRS; MRI; co-registration; aging

Correspondence to: Roee Holtzer, Ph.D., Albert Einstein College of Medicine, Van Etten Building, Room 311, 1225 Morris Park Avenue, Bronx, NY 10461. Tel: 718.430.3962, roee.holtzer@einstein.yu.edu.

Background

Traditional neuroimaging techniques, such as functional magnetic resonance imaging (fMRI), restrict movement and make it difficult to study processes that involve any form of motoric output, such as walking and speaking. An emerging neuroimaging technique called functional near-infrared spectroscopy (fNIRS) addresses this challenge.[1,2] fNIRS is a non-invasive, optical neuroimaging technique that, like fMRI, measures the hemodynamic response. fNIRS is portable, relatively inexpensive, and does not restrict movement. In addition, it provides high temporal resolution and direct measurements of changes in concentrations of blood chromophores, or oxygenated and deoxygenated hemoglobin molecules (oxy-Hb and deoxy-Hb, respectively), which may better elucidate the nature of the hemodynamic response than the fMRI BOLD (Blood-oxygen-level dependent) signal.[3,4]

An fNIRS system contains light sources (i.e. light-emitting diode (LED)) and detectors that cover the scalp. Each source-detector pair creates a “channel” that can be used to monitor the cortical areas that lie around the midpoint between the pair by strategically adjusting the distance between them. In the past two decades, fNIRS has been increasingly used to study various cognitive functions, including but not limited to motor skills,[5,6] vision,[7,8] hearing,[9] speech,[10] social,[11] learning,[12] emotion,[13–15] and executive functions.[16–18] Still, fNIRS is not without its disadvantages. While fNIRS systems vary, compared to fMRI, they typically provide poor spatial resolution of brain regions that are limited by area and depth. Furthermore, there is currently no standard method to register to structural images such as MRI. The lack of spatial information makes interpretation of fNIRS data less meaningful. The current study seeks to address this weakness.

The fNIRS-MRI co-registration literature is scarce.[19] A pioneering study by Okamoto and colleagues proposed a manual projection method,[20] which they used to identify brain coordinates that corresponded to the International 10–20 system positions, an electrode labeling system for EEG (electroencephalography).[21,22] The researchers drew a normal line from each scalp location to the nearest cortical surface. A major limitation of this method was that it was time-consuming and potentially error-prone, emphasizing the need for methods that automatize the process.

The same research team later followed up with a study that examined the utility of automatic projection algorithms[23] and compared their results to those of Okamoto et al.[20] The authors examined three different algorithms and concluded that the balloon-inflation algorithm appeared to be the most efficient and better represented the underlying cortical structure.

Both aforementioned co-registration approaches required individual structural MRIs. Virtual registration methods were later developed to register standalone fNIRS data. These methods utilized a reference database of MRIs and established coordinates of the 10–20 system electrode positions by Okamoto et al.[20,24–27] Virtual registration employs probabilistic registration based on three or four landmark positions on the scalp. It is used in various existing fNIRS software packages, such as HomER2,[28] fNIRS_SPM,[29] POTATo.[30]

To our knowledge, fNIRS-MRI co-registration has never been conducted in older adults; all co-registration studies reviewed thus far included only young and middle-aged adults. This

is a critical limitation because aging has significant effects on brain morphology[31–34] and on functional responses to cognitive task demands.[31,35,36] Specifically, the prefrontal cortex (PFC) deteriorates the most rapidly.[31,34,37–41] This region is associated with executive functions – a number of higher-order cognitive processes that are used to complete complex goal-directed behaviors, such as planning, working memory, attention, reasoning, and problem-solving.[42,43] Recent fNIRS studies have also provided strong evidence for the critical role the PFC plays in cognitive control of mobility in older adults.[44,45] Furthermore, previously established coordinates for fNIRS channels corresponded to the International 10–20 system, which limits the ability to apply those coordinates to more specific brain regions.

To address the limitation mentioned above and fill a critical gap of knowledge in the literature, the current study applied existing co-registration and image-processing methods to co-register fNIRS channels in the PFC to subject-specific structural MRIs in non-demented older adults. The study was designed to provide useful spatial information for standalone fNIRS in future studies for the aging population.

Methods

Participants

A subsample of 37 non-demented older adults from an ongoing cohort study, entitled “Central Control of Mobility in Aging” (CCMA),[46,47] with fNIRS recordings and structural MRI images, was used in the current investigation. The primary aims of the CCMA study are to determine cognitive and brain predictors of mobility in aging. Additional details of the CCMA study design have been reported elsewhere.[46,47] Briefly, CCMA recruited non-demented community-dwelling older adults (age 65+) residing in Yonkers, NY. Prospective participants were first contacted via mail then over the phone. A structured telephone screening interview was administered to potential participants to assess for eligibility. The telephone interview consisted of verbal consent, a brief medical history questionnaire, mobility questions,[48] and validated cognitive screens to exclude dementia.[49,50] General exclusion criteria included severe auditory or visual loss, recent hospitalization that affects mobility, living in a nursing home, serious chronic or acute illness (e.g. cancer), and presence of dementia or other neurodegenerative disease. After completing the telephone interview, eligible individuals were scheduled for two in-person visits at the research center. During the visits, participants received comprehensive neuropsychological, cognitive, psychological, and mobility assessments as well as a structured neurological examination. CCMA participants are followed longitudinally at yearly intervals. Upon the completion of the second study visit, a subset of interested participants was recruited for this study, which involved fNIRS and MRI acquisition. Specific MRI exclusion criteria included left-handedness, claustrophobia, surgically implanted metallic devices (e.g. pacemaker) and presence of neurological gait disorder (e.g. neuropathy). Written informed consent was obtained for each participant during the first in-person visit and approved by the university’s institutional review board. Seven participants were excluded from analysis due to significant shift of fNIRS probe markers. A final sample of 30 participants was used in the current study.

Procedure

fNIRS Acquisition—The fNIRS-1000 imager (fNIR Devices, LLC, Photomac, MD) was used in the current study to assess changes in the hemodynamic activity in the PFC of participants. The fNIRS system consists of a flexible sensor (102gr) that was placed on the participants' forehead using standard procedures, a control box for data acquisition and a computer for data collection and storage. The system can collect data at a sampling rate of 2Hz. The fNIRS sensor consists of 4 LED light sources and 10 photodetectors which cover the forehead using 16 channels, with a source-detector separation of 2.5 cm (see figure 1). The light sources on the sensor (Epitex Inc. type L4X730/4X805/4X850-40Q96-I) contain three built-in LEDs having peak wavelengths at 730, 805, and 850 nm, with an overall outer diameter of 9.2 ± 0.2 mm. The photodetectors (Bur Brown, type OPT101) are monolithic photodiodes with a single supply transimpedance amplifier. The light source emits a ray of light with wavelengths near the infrared spectrum at the scalp. The skin, bone, and nervous tissues are mostly transparent in this spectrum, whereas the oxy-Hb and deoxy-Hb are stronger absorbers of light. After interacting with the chromophores, the light travels back to the detectors on the scalp in a banana-shaped photon path. The concentrations of the chromopores are calculated using the modified Beer-Lambert law[1,2], $I = GI_O e^{-(\alpha_{deoxyHb}C_{deoxyHb}+\alpha_{oxyHb}C_{oxyHb})*L}$, where G is a constant that accounts for measurement geometry, I_O is light source intensity, $\alpha_{deoxyHb}$ and α_{oxyHb} are molar extinction coefficients, and $C_{deoxyHb}$ and C_{oxyHb} are concentrations of deoxy-Hb and oxy-Hb. Light sources and detectors are built on a flexible printed circuit board, which is covered by silicone for sealing, durability, comfort and hygiene. Since the fNIRS sensor is flexible, the components can move and adapt to the various contours of the participants' foreheads, allowing the sensor elements to maintain an orthogonal orientation to the skin surface, improving light coupling efficiency and signal strength. There is a standard sensor placement procedure followed in all of our studies. The fNIRS is placed on the forehead so that the horizontal symmetry axis central (y-axis) coincides with symmetry axis of the head, (i.e. in between the eyes). On the vertical axis, the sensor is positioned right above the eyebrows in relation to the international 10–20 system so that FP1 and FP2 marker locations are approximately positioned on the bottom channel row level[50]. Given the sensitivity of the fNIRS recording device, the lighting in the test room was reduced such that the mean illumination of the forehead was approximately 150 lux, which is about one-third of typical office lighting. Vitamin E capsules were placed on the four corner detectors and four LED light sources in the middle to indicate locations. These markers were later visible on the structural MRI scans.

Structural MRI Acquisition—MRI scanning was performed with a Philips 3T Achieva Quasar TX multinuclear MRI/MRS system equipped with a Dual Quasar High Performance Gradient System, 32-channel broadband digital RF system, Quadrature T/R Head Coil, RapidView reconstructor, Intera Achieva ScanTools Pro R2.5 Package, NetForum and ExamCards, and SENSE parallel imaging capability. T1-weighted whole head structural images were acquired using axial 3D-MP-RAGE parameters over a 240 mm FOV and 1.0 mm isotropic resolution, TE = 4.6 ms, TR = 9.9 ms, α = 8o, with SENSE factor 2.5.

Data Processing and Analysis

Figure 2 summarizes the steps involved in data processing and analysis.

Determination of Channel Locations—On the structural MRI, fiducial markers of the four corner detectors and four middle LED light sources were visible for further processing (see figure 3). Using MRIcron (http://www.mccauslandcenter.sc.edu/mricro/mricron/), implemented with MATLAB R2011b (Mathworks, Natick, MA), the world coordinates (in mm) of the markers were visually obtained from the structural MRI. Then using the fixed distance between each source-detector pair, the unmarked detectors were calculated linearly (see figure 1). If the derived detector location was away from the scalp, the closest point on the scalp was found. The locations of the fiducial markers were chosen to adequately account for the curvature of the forehead while avoiding crowding the MRI scans. The most curved regions on the forehead comprised of the leftmost detectors (i.e., channels 1 and 2) and the rightmost detectors (i.e., channels 15 and 16); these detectors were correctly identified with the vitamin E capsules. The remaining medial detectors lay atop of a relatively flat surface of the forehead; therefore, the detector locations were found by linear interpolation, taking into account of the actual geometry of the source and detector location and separation. Finally, the channel positions on the scalp were calculated as the midpoints of the source-detector pairs.

Reconstruction of Cortical Surface—Using Freesurfer,[51,52] all MRIs were segmented into hemispheres (left, right) and surfaces (gray matter, white matter). The entire pre-processing stream ("Recon-all") was run for all participants. The surface-based segmentation was used to extract surface information for subsequent cortical projection. The program created a mesh of small triangles to represent the brain surface. The vertices of the triangles representing the pia surface (outer layer of gray matter) were extracted, using the Matlab function "read-surf.m," which is included in the Freesurfer software package. The extracted vertices in Freesurfer surface coordinates were then converted to volume (or world) coordinates (in mm; see explanation of coordinate system on Freesurfer website http://surfer.nmr.mgh.harvard.edu/fswiki/CoordinateSystems).

Projection of Channel Location onto Cortical Surface—The cortical projection points of the fNIRS channels were determined using the balloon-inflation algorithm as described in Okamoto & Dan[23] (see figure 4). With the algorithm, 200 points on the cortical surface closest to a point on the scalp were selected, and their centroid was found. Then a virtual rod was passed through the scalp point, through the calculated centroid, to the cortical surface. Three cortical surface points located within the rod were then selected, and their centroid was determined as the final cortical projection point. The virtual rod expanded in radius until the algorithm detected three cortical surface points encapsulated by the rod. The maximum radius was 5 mm. The Matlab function for the algorithm was obtained from the article authors.[23] It utilized the calculated channel coordinates on the scalp and pia surface coordinates obtained from previous steps.

Summation of Group Data—In order to compare different participants, each participant's raw structural MRI was segmented and normalized to an older adult template in

MNI (Montreal Neurological Institute) space, using the Clinical Toolbox for SPM8 (Statistical Parametric Mapping).[53] The older adult template in the Clinical Toolbox was developed based on healthy older adults (mean age 73 years; standard deviation 7.63 years) to replace the standard brain template, which was derived from young adults in SPM8.[54] The toolbox utilized the unified segmentation process of SPM8,[55,56] which included both the segmentation and normalization procedures. The transformation parameters in the normalization process were extracted and applied to each participant's raw cortical projection points using Ged Ridgeway's Matlab function "map_coords" (http://www0.cs.ucl.ac.uk/staff/G.Ridgway/vbm/map_coords.m). Group mean and standard deviation for each x, y, z coordinate were calculated as followed.

$$\text{Mean}=\overline{x},\overline{y},\overline{z}=\frac{\sum x}{n},\frac{\sum y}{n},\frac{\sum z}{n}\quad \text{Standard Deviation}=\sqrt{\frac{\sum(x-\overline{x})^2}{n-1}},\sqrt{\frac{\sum(y-\overline{y})^2}{n-1}},\sqrt{\frac{\sum(z-\overline{z})^2}{n-1}}$$

The MNI coordinates were further normalized to the Talairach brain atlas[57] using Matthew Brett's Matlab function, "mni2tal" (http://imaging.mrc-cbu.cam.ac.uk/imaging/MniTalairach).

Results

Demographics and descriptive information for the 30 participants are summarized in table 1. The mean age in years was 72.73 ± 5.00. Fifty-three percent of participants were female. The low mean disease comorbidity score (GHS = 1.37) confirmed the relatively healthy nature of the sample. The mean RBANS total scaled score (96.80) was indicative of average cognitive function level (43rd percentile).

The group mean cortical projection points expressed in both MNI and Talairach coordinate systems are summarized in table 2. Standard deviations for x, y, and z dimensions are included to represent variability within sample.

Discussion

The goal of this study was to delineate brain morphology of fNIRS channels in the PFC in non-demented older adults. Given that PFC morphology is significantly influenced by aging, fNIRS channel coordinates that were previously established by studies done in younger adults might have limited utility and generalizability to older adult fNIRS data. To our knowledge, this is the first study to determine the spatial correspondence between fNIRS and MRI in this population. We found 16 cortical projection points – points on the cortical surface closest to the fNIRS channel scalp locations – located in the PFC, based on labels probabilistically obtained from the Talairach atlas.[57] The projections points were further inspected visually on an older adult template to ensure accuracy.[54] The standard deviations of the coordinates are all within 10 mm, indicating minimal variability given the spatial resolution of our fNIRS system as permitted by the source-detector distance.

It is to be noted that these points are not precise locations of the fNIRS channel photon path. These are channel locations on the cortical surface without any depth information. Future

studies should use these projection points as anchor points to create regions of interest (ROIs) to capture the fNIRS photon path. Cui et al.[58] explored ROIs of various shapes (single points, spheres, spherical shells, and ellipses) and sizes. They correlated fNIRS signals with mean fMRI BOLD intensities within the ROIs and found that elliptical ROIs yielded the highest correlations. However, adjustments must be made to account for different temporal resolutions in these two modalities.

The cortical projection points are useful to future studies with standalone fNIRS data since individual MRIs are not always available. fNIRS offers critical advantages for research that requires portability, low cost, and higher temporal resolution, especially for studies that aim to determine cortical control of tasks that involve oral, upper limb or lower limb motoric execution. Investigators can better understand their quantitative fNIRS findings with spatial information provided by our study. Our results can also be used as anchor points for virtual probabilistic registration methods.[24–27] These cited papers used Okamoto et al.'s[20] coordinates based on the International 10–20 system electrode locations, which were derived from younger adults' MRIs. In order to capture the true anatomical structures (particularly in the PFC which is most vulnerable to the aging process), future fNIRS investigations in aging would benefit from using the coordinates provided by our study.

Our results provide future investigators added tools to employ fNIRS to study critical age-related processes, particularly ones that are dependent on the PFC. fNIRS measures changes in concentrations of oxy-Hb and deoxy-Hb, which may more directly elucidate the hemodynamic response than fMRI BOLD signals. Since the PFC is particularly sensitive to the effects of aging,[31,34,37–41] the findings reported herein could be utilized by different studies that probe the role of the PFC in distinct cognitive paradigms in older adults. Indeed, a number of studies have demonstrated the usefulness of fNIRS as an instrument to study normal age-related changes in the PFC.[59–65] Consistent with previous findings using other neuroimaging modalities, more diffused activity in the PFC (bilateral) have been found in tasks requiring attention and working memory in older adults, compared to young adults.[61–65] Older adults are also found to recruit bilateral PFC during verbal fluency, which is previously thought to be a left hemisphere process.[59,62–64] These findings suggest functional reorganization of the PFC to counteract anatomical decline.[31,35,36] Recent studies have also used fNIRS to study task-based brain activations associated with gait in older adults, which could not have been directly assessed using less flexible neuroimaging techniques that restricted motion.[44,45] These studies confirmed the role of the PFC in the cognitive control of mobility, especially under conditions involving greater attentional demands (i.e. in dual-task gait conditions).[44,45] Most of the aforementioned studies used approximate brain regions to interpret their standalone fNIRS data. Findings from the current study can help these investigations, as well as future ones, in understanding the quantitative functional results in relation to their structure.

Limitations

This study has several limitations. First, although we aligned the fNIRS sensor with the nasion, the device may have shifted from the intended positions as the participants moved their heads. Second, only some of the fNIRS detectors and light sources were marked with

vitamin-E fiducial markers and other locations were calculated linearly based on fixed distances between each detector-source pair. For future studies, using a 3D digitizer can ameliorate this problem by pinpointing the exact locations of each detector-source pair. Third, similar to other studies, there may be additional errors as result of multiple transformations of the raw data. Finally, this fNIRS-MRI co-registration study excluded left-handed individuals because it utilized data from a larger MRI study, which also involved cognitive tasks. In light of documented structural and functional brain differences between left and right handers,[66,67] whether or not the results of this study will generalize to left-handed participants should be addressed in future research.

Acknowledgments

This research was supported by R01 AG036921 (R. Holtzer, PI) and R01 AG044007 (J. Verghese, PI) NIH/NIA.

References

1. Chance B, Anday E, Nioka S, et al. A novel method for fast imaging of brain function, non-invasively, with light. Opt Express. 1998; 2:411–23. [PubMed: 19381209]
2. Villringer A, Chance B. Non-invasive optical spectroscopy and imaging of human brain function. Trends Neurosci. 1997; 20:435–42. [PubMed: 9347608]
3. Huppert TJ, Hoge RD, Diamond SG, Franceschini MA, Boas DA. A temporal comparison of BOLD, ASL, and NIRS hemodynamic responses to motor stimuli in adult humans. Neuroimage. 2006; 29:368–82. [PubMed: 16303317]
4. Strangman G, Culver JP, Thompson JH, Boas DA. A quantitative comparison of simultaneous BOLD fMRI and NIRS recordings during functional brain activation. Neuroimage. 2002; 17:719–31. [PubMed: 12377147]
5. Leff DR, Orihuela-Espina F, Elwell CE, et al. Assessment of the cerebral cortex during motor task behaviours in adults: a systematic review of functional near infrared spectroscopy (fNIRS) studies. Neuroimage. 2011; 54:2922–36. [PubMed: 21029781]
6. Obrig H, Hirth C, Junge-Hulsing JG, et al. Cerebral oxygenation changes in response to motor stimulation. J Appl Physiol. 1996; 81:1174–83. [PubMed: 8889751]
7. Gratton G, Corballis PM, Cho E, Fabiani M, Hood DC. Shades of gray matter: noninvasive optical images of human brain responses during visual stimulation. Psychophysiology. 1995; 32:505–9. [PubMed: 7568645]
8. Herrmann MJ, Huter T, Plichta MM, et al. Enhancement of activity of the primary visual cortex during processing of emotional stimuli as measured with event-related functional near-infrared spectroscopy and event-related potentials. Hum Brain Mapp. 2008; 29:28–35. [PubMed: 17315227]
9. Zaramella P, Freato F, Amigoni A, et al. Brain auditory activation measured by near-infrared spectroscopy (NIRS) in neonates. Pediatr Res. 2001; 49:213–9. [PubMed: 11158516]
10. Cannestra AF, Wartenburger I, Obrig H, Villringer A, Toga AW. Functional assessment of Broca's area using near infrared spectroscopy in humans. Neuroreport. 2003; 14:1961–5. [PubMed: 14561929]
11. Ruocco AC, Medaglia JD, Tinker JR, et al. Medial prefrontal cortex hyperactivation during social exclusion in borderline personality disorder. Psychiatry Res. 2010; 181:233–6. [PubMed: 20153143]
12. Leon-Carrion J, Izzetoglu M, Izzetoglu K, et al. Efficient learning produces spontaneous neural repetition suppression in prefrontal cortex. Behav Brain Res. 2010; 208:502–8. [PubMed: 20045712]
13. Leon-Carrion J, Damas J, Izzetoglu K, et al. Differential time course and intensity of PFC activation for men and women in response to emotional stimuli: a functional near-infrared spectroscopy (fNIRS) study. Neurosci Lett. 2006; 403:90–5. [PubMed: 16716510]

14. Leon-Carrion J, Martin-Rodriguez JF, Damas-Lopez J, et al. A lasting post-stimulus activation on dorsolateral prefrontal cortex is produced when processing valence and arousal in visual affective stimuli. Neurosci Lett. 2007; 422:147–52. [PubMed: 17601668]
15. Leon-Carrion J, Martin-Rodriguez JF, Damas-Lopez J, et al. Does dorsolateral prefrontal cortex (DLPFC) activation return to baseline when sexual stimuli cease? The role of DLPFC in visual sexual stimulation. Neurosci Lett. 2007; 416:55–60. [PubMed: 17316990]
16. Chance B, Zhuang Z, UnAh C, Alter C, Lipton L. Cognition-activated low-frequency modulation of light absorption in human brain. Proc Natl Acad Sci U S A. 1993; 90:3770–4. [PubMed: 8475128]
17. Leon-Carrion J, Damas-Lopez J, Martin-Rodriguez JF, et al. The hemodynamics of cognitive control: the level of concentration of oxygenated hemoglobin in the superior prefrontal cortex varies as a function of performance in a modified Stroop task. Behav Brain Res. 2008; 193:248–56. [PubMed: 18606191]
18. Nakahachi T, Ishii R, Iwase M, et al. Frontal cortex activation associated with speeded processing of visuospatial working memory revealed by multichannel near-infrared spectroscopy during Advanced Trail Making Test performance. Behav Brain Res. 2010; 215:21–7. [PubMed: 20600348]
19. Tsuzuki D, Dan I. Spatial registration for functional near-infrared spectroscopy: from channel position on the scalp to cortical location in individual and group analyses. Neuroimage. 2014; 85(Pt 1):92–103. [PubMed: 23891905]
20. Okamoto M, Dan H, Sakamoto K, et al. Three-dimensional probabilistic anatomical cranio-cerebral correlation via the international 10–20 system oriented for transcranial functional brain mapping. Neuroimage. 2004; 21:99–111. [PubMed: 14741647]
21. Homan RW, Herman J, Purdy P. Cerebral location of international 10–20 system electrode placement. Electroencephalogr Clin Neurophysiol. 1987; 66:376–82. [PubMed: 2435517]
22. Klem GH, Luders HO, Jasper HH, Elger C. The ten-twenty electrode system of the International Federation. The International Federation of Clinical Neurophysiology. Electroencephalogr Clin Neurophysiol Suppl. 1999; 52:3–6. [PubMed: 10590970]
23. Okamoto M, Dan I. Automated cortical projection of head-surface locations for transcranial functional brain mapping. Neuroimage. 2005; 26:18–28. [PubMed: 15862201]
24. Ayaz H, Izzetoglu M, Platek SM, et al. Registering fNIR data to brain surface image using MRI templates. Conf Proc IEEE Eng Med Biol Soc. 2006; 1:2671–4. [PubMed: 17946973]
25. Singh AK, Okamoto M, Dan H, Jurcak V, Dan I. Spatial registration of multichannel multi-subject fNIRS data to MNI space without MRI. Neuroimage. 2005; 27:842–51. [PubMed: 15979346]
26. Tsuzuki D, Cai DS, Dan H, et al. Stable and convenient spatial registration of stand-alone NIRS data through anchor-based probabilistic registration. Neurosci Res. 2012; 72:163–71. [PubMed: 22062377]
27. Tsuzuki D, Jurcak V, Singh AK, Okamoto M, Watanabe E, Dan I. Virtual spatial registration of stand-alone fNIRS data to MNI space. Neuroimage. 2007; 34:1506–18. [PubMed: 17207638]
28. Huppert TJ, Diamond SG, Franceschini MA, Boas DA. HomER: a review of time-series analysis methods for near-infrared spectroscopy of the brain. Appl Opt. 2009; 48:D280–98. [PubMed: 19340120]
29. Ye JC, Tak S, Jang KE, Jung J, Jang J. NIRS-SPM: statistical parametric mapping for near-infrared spectroscopy. Neuroimage. 2009; 44:428–47. [PubMed: 18848897]
30. Katura T, Sato H, Fuchino Y, et al. Extracting task-related activation components from optical topography measurement using independent components analysis. J Biomed Opt. 2008; 13:054008. [PubMed: 19021388]
31. Cabeza, R., Dennis, NA. Frontal lobes and aging. In: Stuss, DT., Knight, RT., editors. Principles of frontal lobes function. Oxford University Press; New York: 2012. p. 628-52.
32. Craik, FI., Salthouse, TA. The handbook of aging and cognition. Psychology Press; New York and Hove: 2011.
33. Drayer BP. Imaging of the aging brain. Part I. Normal findings. Radiology. 1988; 166:785–96. [PubMed: 3277247]

34. Raz N, Lindenberger U, Rodrigue KM, et al. Regional brain changes in aging healthy adults: general trends, individual differences and modifiers. Cereb Cortex. 2005; 15:1676–89. [PubMed: 15703252]
35. Cabeza R, Anderson ND, Locantore JK, McIntosh AR. Aging gracefully: compensatory brain activity in high-performing older adults. Neuroimage. 2002; 17:1394–402. [PubMed: 12414279]
36. Stern Y. Cognitive reserve. Neuropsychologia. 2009; 47:2015–28. [PubMed: 19467352]
37. Raz N, Gunning FM, Head D, et al. Selective aging of the human cerebral cortex observed in vivo: differential vulnerability of the prefrontal gray matter. Cereb Cortex. 1997; 7:268–82. [PubMed: 9143446]
38. Raz N, Gunning-Dixon FM, Head D, Dupuis JH, Acker JD. Neuroanatomical correlates of cognitive aging: evidence from structural magnetic resonance imaging. Neuropsychology. 1998; 12:95–114. [PubMed: 9460738]
39. Raz N, Rodrigue KM, Haacke EM. Brain aging and its modifiers: insights from in vivo neuromorphometry and susceptibility weighted imaging. Ann N Y Acad Sci. 2007; 1097:84–93. [PubMed: 17413014]
40. West R. In defense of the frontal lobe hypothesis of cognitive aging. J Int Neuropsychol Soc. 2000; 6:727–9. discussion 30. [PubMed: 11011518]
41. West RL. An application of prefrontal cortex function theory to cognitive aging. Psychol Bull. 1996; 120:272–92. [PubMed: 8831298]
42. Ardila A, Rosselli M. Neuropsychological characteristics of normal aging. Developmental Neuropsychology. 1989; 5:307–20.
43. Whelihan WM, Lesher EL. Neuropsychological changes in frontal functions with aging. Developmental Neuropsychology. 1985; 1:371–80.
44. Holtzer R, Mahoney JR, Izzetoglu M, Izzetoglu K, Onaral B, Verghese J. fNIRS study of walking and walking while talking in young and old individuals. J Gerontol A Biol Sci Med Sci. 2011; 66:879–87. [PubMed: 21593013]
45. Holtzer R, Mahoney JR, Izzetoglu M, Wang C, England S, Verghese J. Online fronto-cortical control of simple and attention-demanding locomotion in humans. Neuroimage. 2015; 112:152–9. [PubMed: 25765257]
46. Holtzer R, Mahoney J, Verghese J. Intraindividual variability in executive functions but not speed of processing or conflict resolution predicts performance differences in gait speed in older adults. J Gerontol A Biol Sci Med Sci. 2014; 69:980–6. [PubMed: 24285744]
47. Holtzer R, Wang C, Verghese J. Performance variance on walking while talking tasks: theory, findings, and clinical implications. Age (Dordr). 2014; 36:373–81. [PubMed: 23943111]
48. Baker PS, Bodner EV, Allman RM. Measuring life-space mobility in community-dwelling older adults. J Am Geriatr Soc. 2003; 51:1610–4. [PubMed: 14687391]
49. Galvin JE, Roe CM, Powlishta KK, et al. The AD8: a brief informant interview to detect dementia. Neurology. 2005; 65:559–64. [PubMed: 16116116]
50. Lipton RB, Katz MJ, Kuslansky G, et al. Screening for dementia by telephone using the memory impairment screen. J Am Geriatr Soc. 2003; 51:1382–90. [PubMed: 14511157]
51. Dale AM, Fischl B, Sereno MI. Cortical surface-based analysis. I. Segmentation and surface reconstruction. Neuroimage. 1999; 9:179–94. [PubMed: 9931268]
52. Fischl B, Sereno MI, Dale AM. Cortical surface-based analysis. II: Inflation, flattening, and a surface-based coordinate system. Neuroimage. 1999; 9:195–207. [PubMed: 9931269]
53. Friston KJ, Holmes AP, Worsley KJ, Poline JP, Frith CD, Frackowiak RS. Statistical parametric maps in functional imaging: a general linear approach. Hum Brain Mapp. 1994; 2:189–210.
54. Rorden C, Bonilha L, Fridriksson J, Bender B, Karnath HO. Age-specific CT and MRI templates for spatial normalization. Neuroimage. 2012; 61:957–65. [PubMed: 22440645]
55. Ashburner J, Friston KJ. Nonlinear spatial normalization using basis functions. Hum Brain Mapp. 1999; 7:254–66. [PubMed: 10408769]
56. Ashburner J, Friston KJ. Unified segmentation. Neuroimage. 2005; 26:839–51. [PubMed: 15955494]

57. Talairach, J., Tournoux, P. 3-Dimensional proportional system: an approach to cerebral imaging. Stuttgart: Thieme; 1988. Co-planar stereotaxic atlas of the human brain.
58. Cui X, Bray S, Bryant DM, Glover GH, Reiss AL. A quantitative comparison of NIRS and fMRI across multiple cognitive tasks. Neuroimage. 2011; 54:2808–21. [PubMed: 21047559]
59. Amiri M, Pouliot P, Bonnery C, et al. An Exploration of the Effect of Hemodynamic Changes Due to Normal Aging on the fNIRS Response to Semantic Processing of Words. Front Neurol. 2014; 5:249. [PubMed: 25520697]
60. Beurskens R, Helmich I, Rein R, Bock O. Age-related changes in prefrontal activity during walking in dual-task situations: a fNIRS study. Int J Psychophysiol. 2014; 92:122–8. [PubMed: 24681355]
61. Hagen K, Ehlis AC, Haeussinger FB, et al. Activation during the Trail Making Test measured with functional near-infrared spectroscopy in healthy elderly subjects. Neuroimage. 2014; 85(Pt 1): 583–91. [PubMed: 24045079]
62. Kahlaoui K, Di Sante G, Barbeau J, et al. Contribution of NIRS to the study of prefrontal cortex for verbal fluency in aging. Brain Lang. 2012; 121:164–73. [PubMed: 22285026]
63. Kwee IL, Nakada T. Dorsolateral prefrontal lobe activation declines significantly with age--functional NIRS study. J Neurol. 2003; 250:525–9. [PubMed: 12736729]
64. Scherer LC, Fonseca RP, Giroux F, et al. Neurofunctional (re)organization underlying narrative discourse processing in aging: evidence from fNIRS. Brain Lang. 2012; 121:174–84. [PubMed: 22099970]
65. Vermeij A, van Beek AH, Olde Rikkert MG, Claassen JA, Kessels RP. Effects of aging on cerebral oxygenation during working-memory performance: a functional near-infrared spectroscopy study. PLoS One. 2012; 7:e46210. [PubMed: 23029437]
66. Knecht S, Dräger B, Deppe M, et al. Handedness and hemispheric language dominance in healthy humans. Brain. 2000; 123:2512–8. [PubMed: 11099452]
67. Pujol J, Deus J, Losilla JM, Capdevila A. Cerebral lateralization of language in normal left-handed people studied by functional MRI. Neurology. 1999; 52:1038–43. [PubMed: 10102425]

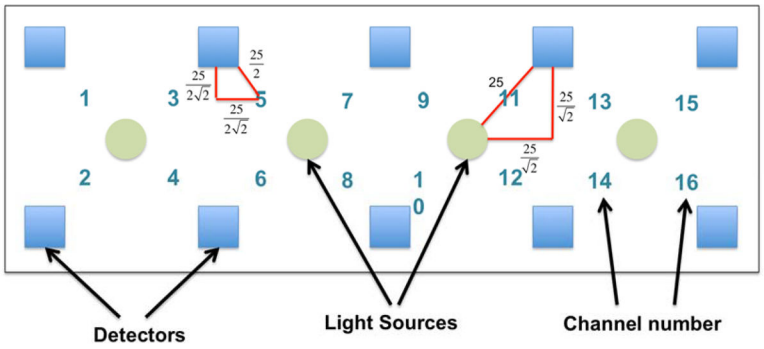

Figure 1.

Depiction of functional near-infrared spectroscopy system

Note. There are 10 detectors (blue squares) and 4 Light Emitting Diode light sources (green circles), creating 16 channels. Each channel is the midpoint of the light source-detector pair. The distance between each detector and light source is 25 mm. Locations of unmarked detectors and channels are derived linearly based on geometric properties.

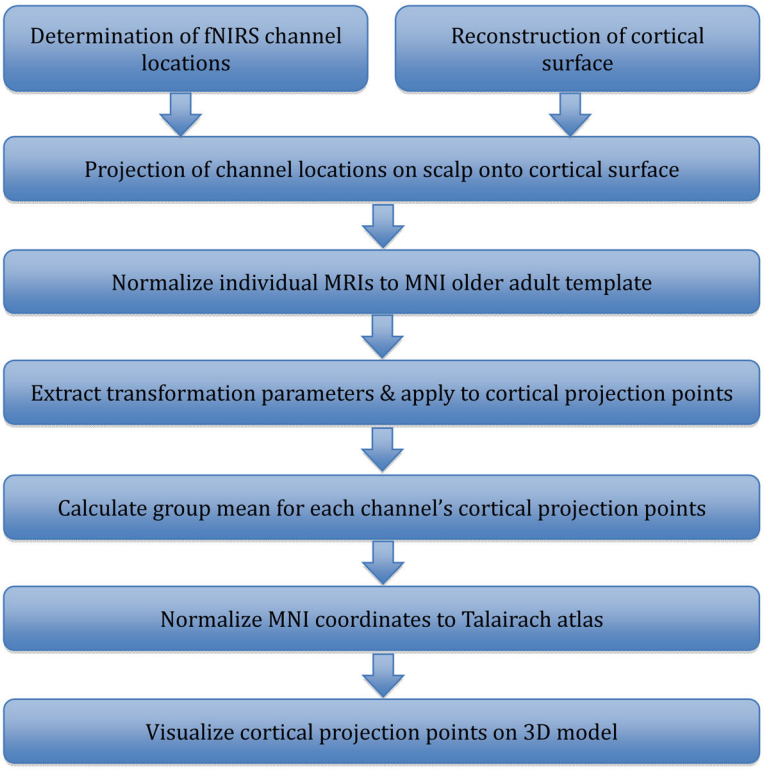

Figure 2.

Summary of co-registration data processing and analysis procedure

Note. fNIRS: functional near-infrared spectroscopy. MNI: Montreal Neurologic Institute.

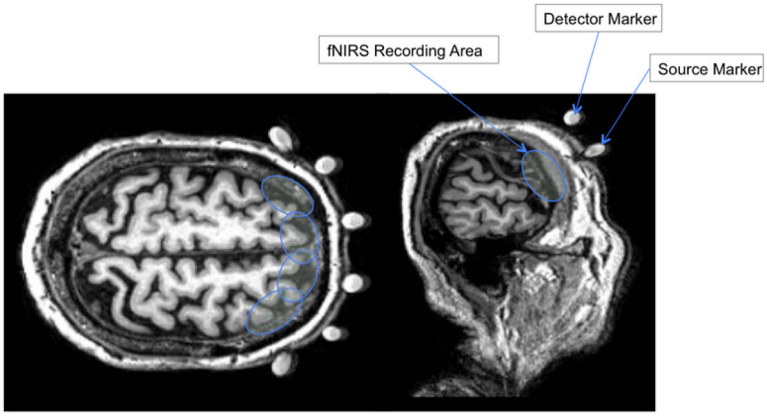

Figure 3.

Anatomical MRIs of fiducial markers

Note. Axial and sagittal MRI slices of a participant. White spheres represent detector and source markers. Blue circles represent possible functional near-infrared spectroscopy recording area by each source-detector pair. The recording regions are estimates, not actual regions.

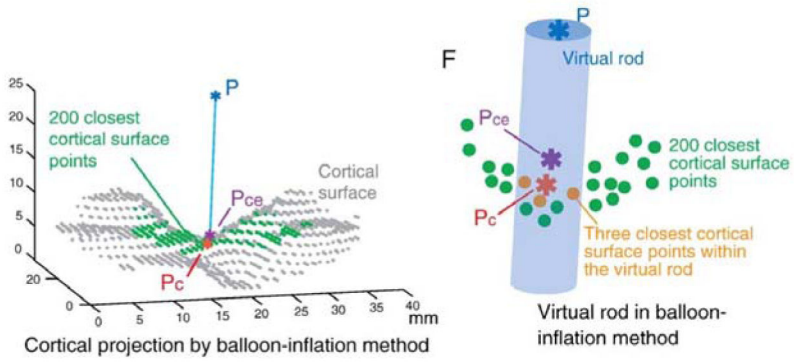

Figure 4.

Balloon-Inflation algorithm

Note. A given point on the scalp (P, blue asterisk) is projected onto the cortical surface (gray dots). The 200 points on the cortical surface closest to P are selected (green dots), and their centroid is found (P_{ce}, purple asterisk). A virtual rod (blue cylinder) is passed from P, through P_{ce}, to the cortical surface (green and gray dots). The three closest cortical surface points within the virtual rod are chosen, and their centroid is determined as the cortical projection point (P_c, orange asterisk). Reprinted from Neuroimage, Vol 26, Okamoto M, Dan I., T Automated cortical projection of head-surface locations for transcranial functional brain mapping, pp 18–28, Copyright (2005),[23] with permission from Elsevier.

Table 1

Descriptive statistics of demographic and screening information (n = 30)

Variables		
Women: number (%)	16 (53.33)	-
	Mean (SD)	Range
Age (years)	72.73 (5.00)	65–81
Education (years)	15.33 (3.10)	12–23
GDS	4.13 (3.15)	0–14
GHS	1.37 (1.07)	0–4
RBANS	96.80 (11.59)	78–119

Note. n: sample size; SD: standard deviation; GDS: Geriatric Depression Scale; GHS: Global Health Score (range 0–10) obtained from dichotomous rating (presence or absence) of diabetes, chronic heart failure, arthritis, hypertension, depression, stroke, Parkinson's disease, chronic obstructive pulmonary disease, angina, and myocardial infarction; RBANS: Repeatable Battery for the Assessment of Neuropsychological Status.

Table 2

Locations of cortical projection points in MNI & Talariach coordinates, split by channel

	MNI Coordinates						Talaraich Coordinates					
Channel	**x**	**SD**	**y**	**SD**	**z**	**SD**	**x**	**SD**	**y**	**SD**	**z**	**SD**
1	−43	4.2	42	4.8	19	8.1	−42	4.2	42	4.4	15	7.6
2	−45	3.7	47	4.5	7	7.6	−45	3.6	46	4.3	5	7.0
3	−36	4.2	53	4.9	16	6.9	−35	4.2	52	4.5	12	6.5
4	−36	4.7	56	4.2	6	7.6	−35	4.6	54	3.9	2	7.0
5	−23	4.2	61	4.2	14	7.1	−23	4.1	60	3.9	10	6.6
6	−23	3.6	63	3.3	5	7.1	−23	3.6	61	3.1	2	6.5
7	−11	4.3	62	4.0	16	6.5	−11	4.3	61	3.7	12	6.1
8	−11	4.2	66	2.7	6	7.7	−11	4.2	64	2.5	3	7.1
9	8	3.9	63	3.6	17	7.3	8	3.9	61	3.3	13	6.9
10	9	4.1	65	3.7	6	7.5	9	4.1	64	3.4	2	7.0
11	21	5.1	61	3.6	16	6.8	21	5.0	60	3.3	11	6.4
12	21	4.3	64	2.6	6	7.6	21	4.3	62	2.3	2	7.0
13	31	5.3	54	5.4	16	7.3	31	5.3	53	5.0	12	6.9
14	33	5.4	57	4.5	6	7.3	32	5.4	55	4.2	3	6.8
15	42	4.1	43	6.2	21	7.1	41	4.1	43	5.8	17	6.8
16	43	4.1	48	5.1	8	6.7	43	4.0	47	4.9	5	6.2

Note. MNI: Montreal Neurologic Institute; SD: standard deviation. All channel values are in mm.

J Neuroimaging. Author manuscript; available in PMC 2018 September 01.